APPLIED ORGANOMETALLIC CHEMISTRY
Appl. Organometal. Chem. **12**, 861–871 (1998)

Diorganotin(IV)–2-Mercaptopyrimidine Complexes

Ralf Schmiedgen,[1] Friedo Huber,[1] Arturo Silvestri,[2] Giuseppe Ruisi,[2] Mario Rossi[2] and Renato Barbieri[2]*
[1]Fachbereich Chemie, Universität Dortmund, Otto-Hahn Str. 6, D-44221 Dortmund, Germany
[2]Dipartimento di Chimica Inorganica, Università di Palermo, Via Archirafi 26–28, I-90123 Palermo, Italy

The complexes formed between the diorganotin(IV) moieties, $R_2Sn(IV)$, and the ligand 2-mercaptopyrimidine, (H)SPym, were investigated. Complexes $R_2SnHal(SPym)$ and $R_2Sn(SPym)_2$ [R = Me, $_i$Pr, $_n$Bu, $_i$Bu, $_t$Bu, cyclohexyl(Cy), Ph] were synthesized, and characterized by elemental analysis. In the solid state, chelation of SPym through S and N donors was established by IR spectroscopy, and the nature of the environment of tin centers was investigated by ^{119}Sn Mössbauer spectroscopy. From the dynamics of ^{119}Sn nuclei determined by variable-temperature measurements on representative compounds [$Me_2SnCl(SPym)$ and $Cy_2SnBr(SPym)$], as well as by point-charge model treatment of nuclear quadrupole splitting parameters, it was inferred that $Me_2SnCl(SPym)$ may assume a *trans*-Me_2 octahedral coordination geometry around tin in a monodimensional polymer, or a monomeric trigonal-bipyramidal structure (distorted). The latter type of structure was assigned to the other $R_2SnHal(SPym)$ species, while $R_2Sn(SPym)_2$ complexes assume a *trans*-octahedral, or skew trapezoidal, tin environment. In $CHCl_3$–$CDCl_3$ solutions, monomeric species occur (according to vapor-pressure osmometry), where ^{1}H and ^{13}C NMR spectroscopic parameters of SPym indicate the persistence of Sn chelation by S and N donor atoms. The $Me_2SnCl(SPym)$ species assume trigonal-bipyramidal structures with a chelating SPym ligand, in $CDCl_3$ and C_2H_5OH solutions, according to the coupling constants $^1J(^{119}Sn,^{13}C)$, as well as IR and ^{119}Sn Mössbauer spectroscopic data. ^{119}Sn NMR parameters fully correspond with data for the homologous complexes with 2-mercaptopyridine. © **1998 John Wiley & Sons, Ltd.**

Keywords: diorganotin; Pyrimidine; complex; Mössbauer; IR; NMR

Received 26 January 1998; accepted 4 May 1998

* Correspondence to: Professor Renato Barbieri, Dipartimento di Chimica Inorganica, Università di Palermo, Via Archirafi 26–28, I-90123 Palermo, Italy.
Contract/grant sponsor: Ministero per l'Università e la Ricerca Scientifica (Roma).
Contract/grant sponsor: Fonds der Chemischen Industrie.
Contract/grant sponsor: European Community.

INTRODUCTION

Continuing our studies on tin(IV) coordination by thiol sulfur, we have recently investigated, *inter alia*, bonding and structure in a series of monoorganotin(IV) complexes with 2-mercaptopyrimidine, (H)SPym, i.e. $RSn(SPym)_3$, $RSnCl(SPym)_2$, $RSnCl_2(SPym)$ (R = alkyl, aryl), as well as in $SnCl_2(SPym)_2$ and $Sn(SPym)_4$;[1] evidence was obtained for tin chelation by thiol sulfur and one heterocyclic nitrogen atom[1] (Fig. 1), in line with the crystal and molecular structure (by X-ray diffractometry) of *n*$BuSn(SPym)_3$[2] as well as with the dynamics of tin nuclei in $MeSnCl(SPym)_2$, $SnCl_2(SPym)_2$ and $Sn(SPym)_4$ as determined by variable-temperature ^{119}Sn Mössbauer spectroscopy.[3] The second nitrogen atom of the $^-$SPym ligand (Fig. 1) in the complexes mentioned above is not involved in coordination to tin.[1–3]

The studies have been extended to $^-$SPym complexes of $R_2Sn(IV)$ moieties, $R_2SnCl(SPym)$ and $R_2Sn(SPym)_2$; the results obtained are reported in the present paper, and discussed in relation to earlier work on $R_2Sn(SPym)_2$[4] and $R_2SnCl(SPy)$[5] and $R_2Sn(SPy)_2$[5] complexes [(H)SPy = 2-mercaptopyridine)].

Metal coordination by $^-$SPym is of some biochemical interest. In fact, the presence of 2-mercaptopyrimidine nucleotides has been detected, e.g. in *E. coli* sRNA and yeast tRNA, and

 CCC 0268–2605/98/120861–11 $17.50

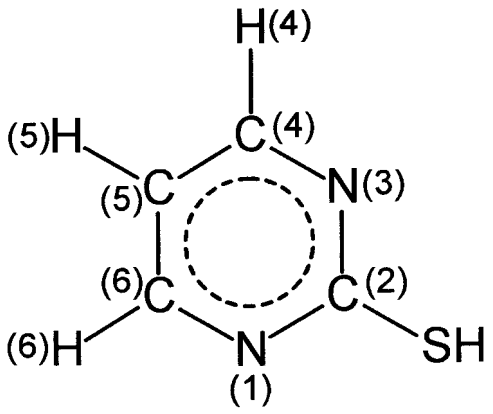

Figure 1 2-Mercaptopyrimidine, thiol conformer: labeling for NMR assignments.

participate in hydrogen bonds in the nucleic acid.[6–9] Due to the large stability constants of $R_nSn–S_{thiol}$ complexes, e.g. for $Me_3Sn(IV)$,[10] bonding of organotins to these thiolated nucleotides would be expected in biological systems. Moreover, coordination of $R_nSn(IV)$ moieties by thiolated ligands is expected to reduce the physiological action of organotins, as detected for e.g. the antitumor activity *in vitro* of $R_2Sn(SPy)_2$ complexes.[11]

EXPERIMENTAL

Diorganotin(IV) dihalides were synthesized by literature methods.[12–15] (H)SPym was a product from Fluka Chemie AG. Other reagents and solvents were commercial products which were purified and dried according to standard procedures.[16] Syntheses were effected in a dry nitrogen atmosphere, under stirring and using dried solvents. Methods employed in the synthesis of $R_2SnHal(SPym)$ and $R_2Sn(SPym)_2$ complexes, Table 1, were as follows.

(A) R_2SnCl_2 in $CHCl_3$ solution [4 mmol for the synthesis of $R_2SnCl(SPym)$; [2 mmol for $R_2Sn(SPym)_2$] was added to 4 mmol of NaSPym in $CHCl_3$–CH_3OH; the procedure reported in Ref.

Table 1 Analytical data for diorganotin(IV)-2-mercaptopyrimidine complexes

Compound[a]		Method[a] and yield	M.	Mol. wt.[c] Found	Analytical data: Found (calcd)%			
No.	Formula	(%)	(°C)[b]	(calcd)	C	H	N	Hal
1	$Me_2SnCl(SPym)$	A 75	147(dec.)	306 (295.36)	24.2 (24.4)	3.0 (3.1)	9.4 (9.5)	11.9 (12.0)
2	$_iPr_2SnCl(SPym)$	B 99	120	365 (351.47)	33.2 (34.2)	4.9 (4.9)	7.7 (8.0)	10.2 (10.1)
3	$_nBu_2SnCl(SPym)$	A 62	62	383 (379.52)	37.5 (38.0)	5.5 (5.6)	7.3 (7.4)	9.2 (9.3)
4	$_iBu_2SnCl(SPym)$	A 89	122	373 (379.52)	37.7 (38.0)	5.8 (5.6)	7.4 (7.4)	9.2 (9.3)
5	$_tBu_2SnCl(SPym)$	A 46	197(dec.)	369 (379.52)	38.2 (38.0)	6.0 (5.6)	7.5 (7.4)	9.4 (9.3)
6	$Cy_2SnCl(SPym)$	C 77	209(dec.)	448 (431.60)	44.3 (44.5)	6.0 (5.8)	6.5 (6.5)	8.3 (8.2)
7	$Cy_2SnBr(SPym)$	A 75	200	485 (476.05)	40.2 (40.4)	5.4 (5.3)	5.8 (5.9)	17.1 (16.8)
8	$Ph_2SnCl(SPym)$	D 74	115	431[d] (419.50)	45.8 (45.8)	3.0 (3.1)	6.7 (6.7)	8.6 (8.5)
9	$Me_2Sn(SPym)_2$	A 59	239(dec.)[e]	366 (371.05)	31.8 (32.4)	3.2 (3.3)	14.8 (15.1)	—
10	$_iPr_2Sn(SPym)_2$	A 65	223	449 (427.16)	39.2 (39.4)	4.9 (4.7)	13.0 (13.1)	—
11	$_nBu_2Sn(SPym)_2$	A 57	158[f]	443 (455.21)	42.8 (42.2)	5.4 (5.3)	12.6 (12.3)	—
12	$_iBu_2Sn(SPym)_2$	A 72	196	458 (455.21)	41.7 (42.2)	5.4 (5.3)	11.8 (12.3)	—
13	$_tBu_2Sn(SPym)_2$	A 74	211	465 (455.21)	41.6 (42.2)	5.3 (5.3)	12.2 (12.3)	—
14	$Cy_2Sn(SPym)_2$	A 65	263(dec.)	480 (507.29)	48.0 (47.4)	5.9 (5.6)	11.1 (11.0)	—
15	$Ph_2Sn(SPym)_2$	A 81	216[g]	485[h] (495.19)	48.0 (48.5)	3.2 (3.3)	11.2 (11.3)	—

[a] HSPym = 2-mercaptopyrimidine, $C_4H_3N_2SH$; thiol conformer in Fig. 1. Me = methyl; Pr = propyl; Bu = butyl; Cy = cyclohexyl; Ph = phenyl; *n* = normal; *i* = iso; *t* = tertiary. Methods of synthesis are described in the Experimental section. Data for **1** refer to a representative synthetic batch (see Table 3 and text). % S found (calcd): (**1a**) 11.2 (10.9); (**1c**) 11.35 (10.9); (**2**) 9.2 (9.1); (**3**) 8.7 (8.5); (**4**) 9.5 (8.5); (**5**) 8.8 (8.5); (**7**) 6.9 (6.7); (**8**) 7.98 (7.6); (**9**) 17.1 (17.3); (**10**) 15.2 (15.0); (**12**) 14.6 (14.1); (**13**) 14.3 (14.1); (**14**) 12.4 (12.6); (**15**) 13.5 (13.0).
[b] Dec. = melting with decomposition. Uncorrected data.
[c] Determined by vapor pressure osmometry in $CHCl_3$ solutions.
[d] Mol.wt = 466 in dimethyl sulfoxide (DMSO) solutions.
[e] Ref. 5: m.pt = 247 °C.
[f] Ref. 5: m.pt = 161 °C.
[g] Ref. 5: m.pt = 196 °C.
[h] Mol.wt. = 501 in DMSO.

Table 2 Infrared spectral data for diorganotin(IV) complexes of 2-mercaptopyrimidine:[a] collective ranges of values[b] (cm^{-1})

		ν(C–N/C–C)			δ(C–H)[c]			Ring[d]
Compd	Formula[a]	A	B	C	D	E	F	G
1–8	$R_2SnHal(SPym)$[e]	1566–1576 (vs, s, m)	1546–1549 (vs, s)	1366–1386 (vs, s)	800–821 (s, m, w)	769–773 (vs, s, m)	748–749 (vs, s, m, w)	645–649 (vs, s, m)
9–15	$R_2Sn(SPym)_2$[f]	1560–1565 (vs, s, m)	1541–1545 (vs, s)	1361–1378 (vs, s, sh)	794–807 (s, m, w)	770–775 (s, m, w)	746–748 (vs, s, m)	638–641 (vs, s, m)

[a] Solid-state samples. Structure of 2-mercaptopyrimidine in Fig. 1. R, Hal in classes of complexes: see Table 1.
[b] Determined in Nujol mulls, between KBr discs; s = strong, v = very, m = medium, w = weak, sh = shoulder. A–G: classes of vibrational bands.
[c] Out-of-plane deformation.
[d] Ring deformation.
[e] Compound **1** $CDCl_3$ solution in KBr cuvettes: A, 1572 vs; B, 1550 vs; C, 1381 vs.
[f] Vibrational data for Nos **9, 11, 15** (see Table 1), reported in Ref. 4, essentially insert into the ranges reported here.

5, Method A (preparation of SPy complexes) was followed. After stirring at room temperature, the solvent was removed at 20 °C, and the residue extracted with $CHCl_3$. Upon addition of petroleum ether, the product was obtained by crystallization at −30 °C.[5]

(B) $^{i}Pr_2Sn(SPym)_2$ was reacted with $^{i}Pr_2SnCl_2$ (1:1) in $CHCl_3$ solution, according to Ref. 5, method D.

(C) Analogous to method A above, with the difference that the extract was taken to dryness (Ref. 5, method B).

(D) $Ph_2Sn(SPym)_2$ 1 mmol was reacted with 1 mmol of Ph_2SnCl_2 in 50 ml of CCl_4 under reflux for 24 h. The solvent was then removed in a rotary evaporator, the solid product obtained was treated with 10 ml of Et_2O, filtered off and dried under vacuum.

Elemental analyses for C, H, N were effected by a 1106 analyzer (Carlo Erba, Milano, Italy). Data for S (Table 1, footnote a) were determined at the Department of Inorganic, Organometallic and Analytical Chemistry, University of Padova, Italy. The analysis of halogens was carried out by potentiometry, following reaction of the complexes with sodium peroxide and ethylene glycol in a Parr bomb.[17] Melting points were measured with a Büchi SMP 20 instrument, and decomposition temperatures by DTA/TG employing a Mettler vacuum thermoanalyzer T1 (reference: Al_2O_3, 25 °C; N_2, 6 °C min^{-1}; Pt/PtRh thermoelement). Molecular weights were measured by a Knauer vapor-pressure osmometer. The IR spectra were taken by a Bruker FTIR IFS 113V spectrometer for solid samples (KBr pellets), and by a Perkin-Elmer PE 580B grating instrument for solutions (cell with KBr windows, 25 μm). ^{119}Sn Mössbauer spectra were measured, at liquid-nitrogen temperature (solid or frozen solution absorbers) as well as in variable-temperature experiments, by the apparatus and procedures previously reported.[18,19] NMR spectra were determined by Bruker AM 300 or Bruker AC 200 spectrometers at 37 °C.

RESULTS AND DISCUSSION

The analytical data in Table 1 are fully consistent with the stoichiometries $R_2SnHal(SPym)$ (complexes **1–8**) and $R_2Sn(SPym)_2$ (complexes **9–15**). Results of elemental analyses for complexes **1**, $Me_2SnCl(SPym)$, obtained from a series of synthetic batches (Table 3, below), corresponded to the data in Table 1. The occurrence of monomeric, undissociated, species in $CHCl_3$ solutions (as well as in dimethyl sulfoxide (DMSO) for **8** and **15**) is generally inferred from the osmometric data.

Complexes **1–15** are colorless or light-yellow solids, which when stored at 0 °C did not show any decomposition over several months. The compounds are soluble in $CHCl_3$ and DMSO, and moderately soluble in CH_3OH and C_2H_5OH.

The infrared spectra of the solid-state complexes **1–15** (Table 2) correspond strictly[1] to literature data determined for $RSn(SPym)_3$, $RSnCl(SPym)_2$, $RSnCl_2(SPym)$, $SnCl_2(SPym)_2$ and $Sn(SPym)_4$, which have been interpreted in terms of the occurrence of chelation of tin centers by N and S donors of the SPym ligands.[1] The same would then be inferred for the $R_2Sn(IV)$–SPym complexes investigated here, according to earlier assumptions for $R_2Sn(SPym)_2$ species (R = Me, ^{n}Bu, Ph).[4]

Table 3 ^{119}Sn Mössbauer parameters of diorganotin(IV)-2-mercaptopyrimidine complexes

Compound[a]				
No.	Formula	δ[b] (mm s^{-1})	ΔE[c] (mm s^{-1})	$\Gamma_1;\Gamma_2$[d] (mm s^{-1})
	Solid state			
1a	$Me_2SnCl(SPym)$	1.43	3.22	0.83
		1.427 ± 0.003[e]	3.202 ± 0.007[e]	0.900 ± 0.038[e]
1b	$Me_2SnCl(SPym)$	1.48	3.39	0.96
1c	$Me_2SnCl(SPym)$	1.47	3.53	0.92
		1.455 ± 0.004[e]	3.471 ± 0.009[e]	0.895 ± 0.017[e]
2	$_i Pr_2SnCl(SPym)$	1.65	3.19	0.92
3	$_n Bu_2SnCl(SPym)$	1.49	3.08	0.92
4	$_i Bu_2SnCl(SPym)$	1.50	3.01	0.83
5	$_t Bu_2SnCl(SPym)$	1.73	3.08	0.93
7	$Cy_2SnBr(SPym)$	1.65	3.10	0.90; 0.87
		1.694 ± 0.004[e]	3.155 ± 0.010[e]	0.851 ± 0.027; 0.883 ± 0.035[e,f]
8	$Ph_2SnCl(SPym)$	1.31	2.53	0.83
9	$Me_2Sn(SPym)_2$	1.32	2.47	1.02
		1.30[g]	2.46[g]	0.91[g]
10	$_i Pr_2Sn(SPym)_2$	1.65	2.86	0.82
11	$_n Bu_2Sn(SPym)_2$	1.51	2.87	0.79
		1.51[g]	2.90[g]	1.00[g]
12	$_i Bu_2Sn(SPym)_2$	1.51	2.77	0.79
13	$_t Bu_2Sn(SPym)_2$	1.71	2.73	1.12
14	$Cy_2Sn(SPym)_2$	1.63	2.93	0.97
15	$Ph_2Sn(SPym)_2$	1.36	2.53	0.80
		1.27[g]	2.53[g]	1.04[g]
	Frozen ethanol solutions.			
1b	$Me_2SnCl(SPym)$[h]	1.23	3.15	0.99
1c	$Me_2SnCl(SPym)$[i]	1.39	3.29	0.85

[a] Abbreviations: see footnote a to Table 1. Nos **1a–1c:** samples from different synthetic batches; analytical data and mol.wts correspond to the representative values in Table 1.
[b–d] Determined at 77.3 K (unless otherwise stated) on finely powdered solid absorber samples, or in frozen solutions. Average values for data determined on samples from individual synthetic batches are generally quoted.
[b] Isomer shift with respect to room-temperature $Ca^{119}SnO_3$.
[c] Nuclear quadrupole splitting.
[d] Full width at half height of the resonant peaks at higher and lower velocity than the spectrum centroid respectively; spectra with $\Gamma_1 = \Gamma_2$ were fitted as symmetrical doublets with the NORMOS program.
[e] Values of hyperfine parameters from variable-temperature Mössbauer spectroscopy experiments (Table 4) Data averaged over the whole temperature ranges, with standard error.
[f] Slightly asymmetric peaks; fitting with two linewidth values.
[g] Data from Ref. 4.
[h, i] Approx. 2 ml of solutions in polyethylene samples holders, frozen by immersion in liquid N_2; (h) 6.8 mM and (i) 7.1 mM solutions.

The structure of the bonding environment of tin atoms may be extracted from ^{119}Sn Mössbauer spectroscopy parameters.[20–22] The data inherent to the complexes investigated here are reported in Table 3, and the results of studies on the dynamics of tin nuclei by variable-temperature Mössbauer spectroscopy (vtMs)[23–25] are given in Table 4 and Figs 2, 3 and 4. The quality of the measured spectra is shown in Fig. 2. By fingerprint, from the values in Table 3 it is inferred that: (i) the isomer shift parameters, δ, lie in the zone for $R_2Sn(IV)$ species;[20–22] and (ii) the quadrupole splitting parameters, ΔE, are within ranges typical for trigonal-bipyramidal and *trans*-R_2 octahedral $R_2Sn(IV)$ derivatives.[20–22] Comparison of the δ and ΔE values for the SPym complexes in Table 3 with data inherent to complexes of $R_2Sn(IV)$ moieties with ligands L characterized by S_{thiol} and N_{het} donor atoms, belonging to the same class as $^-$SPym, shows the general correspondence between values, as well as between ΔE parameters of $R_2Sn(SPym)_2$ and -$(L)_2$, and $Ph_2SnCl(SPym)$ and -(L) [L = anions of 2-mercaptopyridine (SPy); 2-mercaptopyridine-5-carboxylic acid, methyl, ethyl

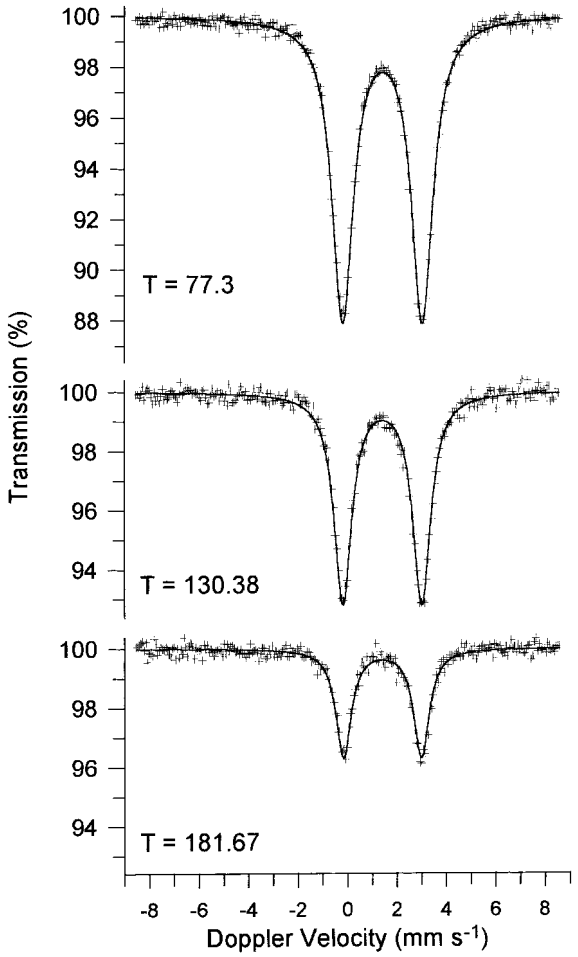

Figure 2 The quality of ^{119}Sn Mössbauer spectra: data for $Me_2SnCl(SPym)$, **1a** (see Tables 3 and 4).

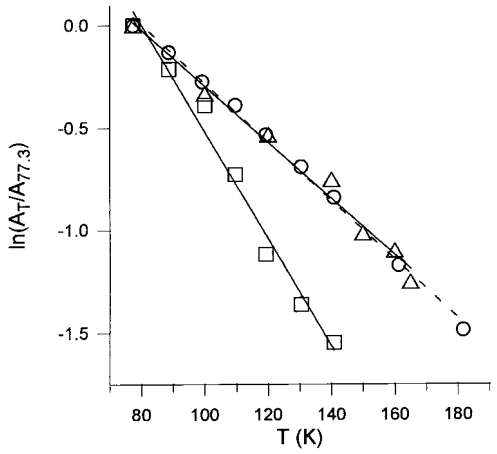

Figure 3 Temperature dependence of the normalized total Lorentzian areas, *A*, under the ^{119}Sn Mössbauer peaks for: (○) $Me_2SnCl(SPym)$ (**1a**), (△) $Me_2SnCl(SPym)$ (**1c**), (□) $Cy_2SnBr(SPym)$ (**7**). See Table 4. Lines are the least-squares fits to the experimental data points, the related expressions for ln ($A_T/A_{77.3}$) being as follows: $1.148 - 1.430 \times 10^{-2}\ T$ (○); $1.073 - 1.370 \times 10^{-2}\ T$ (△); $2.086 - 2.605 \times 10^{-2}\ T$ (□).

and isopropyl esters (TNME, TNEE, TNIPE); 2-thiocytosine (TCy); 8-thioquinoline (TOx): $R_2SnHal(L)$, R = alkyl, phenyl: δ = 1.22–1.71 mms^{-1} [3,5,9,24–26]

$R_2Sn(L)_2$, R = alkyl, phenyl; δ = 1.30–1.71 mms^{-1}

$Alk_2Sn(L)_2$: ΔE = 2.55–2.95 mms^{-1}

$Ph_2Sn(L)_2$: ΔE = 2.30–2.40 mms^{-1}

$Ph_2SnCl(L)$: ΔE = 2.35–2.58 mms^{-1}

In contrast, the magnitude of ΔE values for $Alk_2SnCl(SPym)$, particularly for Alk = CH_3 (Table 3), are consistently larger than data for $Alk_2SnHal(L)$, ΔE = 2.78–3.03 mms^{-1} [3,5,26]

It should then be concluded that $Ph_2SnCl(SPym)$ assumes the trigonal-bipyramidal (distorted) structure which has been determined by X-ray crystallography for $Ph_2SnCl(SPy)$[5,27] and $Ph_2SnCl(TNEE)$,[27] as well as for $Bz_2SnCl(TOx)$;[29] moreover, the structures of the $R_2Sn(SPym)_2$ complexes listed in Table 3 would correspond to the *trans*-octahedral (or *skew*-trapezoidal, sometimes defined also as distorted tetrahedral) X-ray structures reported for $Me_2Sn(SPy)_2$,[30] Me_2Sn- and $_nBu_2Sn$-$(TNEE)_2$,[31,32] $_nBu_2Sn(SPy\text{-}5\text{-}NO_2)_2$,[33] $Cy_2Sn(SPy)_2$[11] and $Ph_2Sn(SPy)_2$.[34] According to the magnitude of the ^{119}Sn Mössbauer parameters ΔE (Table 3), the complexes $Alk_2SnHal(SPym)$ (**1–7**) would instead assume structures differing from those reported for $Me_2SnCl(TNEE)$ and $Et_2SnBr(TNIPE)$, which show distorted tbp tin environments according to X-ray crystallographic data;[26] the largest structural difference would concern the complex $Me_2SnCl(SPym)$.

The ^{119}Sn Mössbauer parameters of the latter species, **1a–1c** in Table 3, show several interesting features. Samples **1a, 1b, 1c** refer to independent synthetic batches, effected in order to check stoichiometries and properties of the product. In all cases the same compound was obtained, as shown by the analytical data (Table 1); the practically constant isomer shifts, δ, and linewidths, $\Gamma_{1,2}$, which are narrow enough to allow fitting of the experimental peaks with only one doublet, indicating a single type of tin coordination environment. On the other hand, the quadrupole splitting parameters (ΔE) vary within about 0.3 mms^{-1},

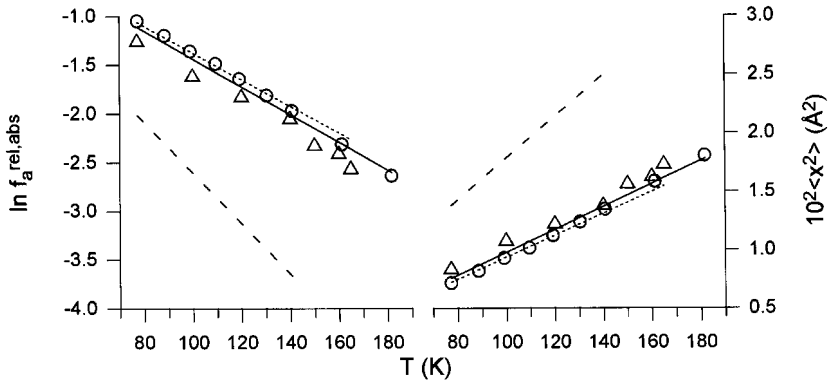

Figure 4 The recoil-free fraction of absorber ^{119}Sn nuclei, f_a, and the mean square displacement of ^{119}Sn, $< x^2 >$, as functions of temperature. Lines are $f_a^{rel}(T)$ and $< x^2 >$ functions extracted from slopes d(ln *A*)/d*T* (Table 4 and text); data points are f_a^{abs} and corresponding $< x^2 >$ values. —— ○, $Me_2SnCl(SPym)$ (**1a**); …… △, $Me_2SnCl(SPym)$ (**1c**); - - - - $Cy_2SnBr(SPym)$ (**7**); see Table 4.

which would suggest variations, although limited, in the structures.

The only structural feature possibly yielding increases in $|\Delta E|$ is the enlargement of C-Sn-C angles,[21,35] other parameters being constant (e.g. angles S-Sn-N and S-Sn-Cl, taken from Me_2SnCl(TNEE) and Et_2SnBr(TNIPE))[26]. Possibly the increase of C-Sn-C reflects the coordination to tin by N(3) of 2-mercaptopyrimidine (Fig. 1) thus obtaining monodimensional polymeric species with octahedral-type tin environments. In order to check the latter hypothesis, vtMs measurements[23–25] have been performed, and the results are reported in Table 4 and Figs 3 and 4; samples of $Me_2SnCl(SPym)$ with the lesser and larger ΔE at 77.3 K, **1a** and **1c** (Table 3) have been selected, and the complex $Cy_2SnBr(SPym)$ (**7**), with a lower ΔE, has been investigated for comparison purposes. From vtMs parameters and functions it is inferred that:[3,19,36]

(i) δ and ΔE parameters are practically invariant in the temperature ranges investigated (Tables 3 and 4) which rules out the occurrence of phase transitions as well as of second-order Doppler shifts;
(ii) areas under the resonant peaks are symmetric at each temperature for **1a, 1c**, which indicates isotropic lattice dynamics of the recoil-free fraction (see for example Fig. 2); the reverse would occur for **7**, as inferred from asymmetric areas (see for example Γ_1, Γ_2 in Table 3);

Table 4 ^{119}Sn dynamics data functions from variable-temperature Mössbauer spectroscopy (vtMs)

Compound		Sample thickness	10^2d(ln *A*)/d*T*[c]	ϑ_D[d]	$\tilde{\nu}_D$[d]		Temp. range
No.[a]	Formula[b]	(mg ^{119}Sn cm^{-2})	(K^{-1})	(K)	(cm^{-1})	$10^{-6}M\,\vartheta_D^{2e}$	(K)
1a	$Me_2SnCl(SPym)$	0.97(6)	−1.430 (0.998)	71.0 (72.2)	49.3 (50.1)	1.49 (1.54)	77.3–181.7
1c	$Me_2SnCl(SPym)$	0.67	−1.370 (0.993)	72.6 (68.6)	50.4 (47.7)	1.56 (1.39)	77.3–165.0
7	$Cy_2SnBr(SPym)$	0.46	−2.605 (0.991)	41.4 (50.5)	28.8 (35.1)	0.82 (1.22)	77.3–140.8

[a] See Table 3.
[b] Abbreviations: see footnote a to Table 1.
[c] $A = (\pi/2)\,\varepsilon\,\Gamma$ mm s^{-1}, is the total (Lorentzian) area under the resonant peaks, ε% being the resonant effect; correlation coefficients in parentheses.
[d] Debye temperature, ϑ_D, and cut-off frequency, $\tilde{\nu}_D$, calculated from d(ln *A*)/d*T*, assuming the molecular mass of the complex to be the vibrating mass.
[e] Parameter of intermolecular force constant; *M* = molecular mass (amu).
[d,e] 'Absolute' data are in parentheses (see text).

(iii) the narrowness of the Γ values throughout the temperature range (Table 3), and the lack of discontinuities for functions $A(T)$ (Fig. 3), indicate the occurrence of single solid-state phases in each complex, as well as harmonic motions of Sn nuclei, at least in **1a, 1c.**

Consequently, the following fingerprint criteria may be accounted for:

(a) Slopes d(ln A)/dT (K^{-1}) for $R_2Sn(IV)$ derivatives:[36] border zone -1.63×10^{-2} to -1.69×10^{-2} K^{-1}; polynuclear species in the range -0.49×10^{-2} to -1.63×10^{-2} K^{-1} (where five mononuclear species are also located, possibly characterized by weak intermolecular bonding, within a total of 26 compounds[36]); mononuclear species, -1.69×10^{-2} to -2.87×10^{-2} K^{-1} (one polynuclear species among nine compounds[36]); the border zone could be then extended to the range -1.20×10^{-2} to -1.95×10^{-2} K^{-1}.[22,36]
(b) Debye temperature, ϑ_D:[37] 21.6–68.5 K for mononuclear; 58.6–105.7 K for polynuclear species.
(c) Parameter of the intermolecular force constant, $M\vartheta_D^2$:[37] 0.74×10^6–1.77×10^6 for mononuclear; 1.07×10^6–3.24×10^6 for polynuclear; 1.07×10^6–1.60×10^6 for polynuclear, monodimensional species.
(d) Functions $<x^2>/T$, where $<x^2>$ is the mean square displacement of Sn atoms:[38] borderline is located at $<x^2>$ $\approx 0.8 \times 10^{-2}$ Å^2 (T = 77.3 K); $\approx 2.0 \times 10^{-2}$ Å^2 (T = 200 K); $\approx 2.8 \times 10^{-2}$ Å^2 (T = 280 K).

On these grounds, the following conclusions could be drawn for compounds $Me_2SnCl(SPym)$, **1a, 1c** and $Cy_2SnBr(SPym)$ (**7**) from the data in Table 4 and Fig. 4: *$Me_2SnCl(SPym)$:* polynuclear from d(ln A)/dT and ϑ_D; polynuclear (monodimensional) or mononuclear from $M\vartheta_D^2$ and $<x^2>(T)$; *$Cy_2SnBr(SPym)$:* essentially mononuclear from all parameters and functions

The vtMs parameters and functions inherent to the homologous complexes $Me_2SnCl(TOx)$ and $Me_2Sn(TUr)$ (TUr = 2-thiouracil) lie in the zone for mononuclear, or borderline, species,[3] although $^nBu_2Sn(TUr)$ has been assigned a polymeric structure from IR studies.[39] Moreover, vtMs parameters for $Me_2Sn(TCy)_2$, which is expected to assume a monomeric *trans*-Me_2 octahedral-type structure,[3] correspond to values reported for $Me_2SnCl(TOx)$ and $Me_2Sn(TUr)$.[3] On the other hand, $nBu_2Sn(SPym)_2$ shows[4] d(ln A)/dT = -1.4×10^{-2} K^{-1}, which surprisingly corresponds to data for $Me_2SnCl(SPym)$ in Table 4. Complexes $Me_2SnCl(SPym)$ behave as Debye solids, as shown by the correspondence of parameters and functions (Table 4 and Fig. 4) extracted from the slopes d(ln A)/dT ('relative'), as well as from the recoil-free fraction of the source ('absolute').[3,36] The latter does not hold for $Cy_2SnBr(SPym)$, as shown for example by the large difference between relative and absolute values[3,36] of ϑ_D and $\tilde{\nu}_D$ in Table 4.

From the dynamics of ^{119}Sn nuclei, a *trans*-R_2 octahedral-type structure in a monodimensional polymer would then be inferred, at least for $Me_2SnCl(SPym)$, since the limited increments of ΔE from **1a–1c** (Table 3) are paralleled by analogous changes in vtMs parameters and functions towards data for polynuclear species (Table 4).

Assignment of the structure of tin environments by calculations of ΔE according to the point-charge model formalism[20–22] is attempted here for both *trans*-R_2 octahedral and trigonal-bipyramidal configurations according to the rule by Clark *et al.*,[40] $(|\Delta E_{exp}| - |\Delta E_{calcd}|) \leq 0.4$ mms^{-1}. Partial nuclear quadrupole splitting parameters reported in the literature[3,5] are employed in the estimates of ΔE_{calcd}; ΔE_{exp} data for ^-SPym complexes are from Table 3, while data for $R_2SnHal(L)$ and $R_2Sn(L)_2$ have been listed above. The occurrence of regular (idealized) tin environments is assumed first; the following would be inferred:

(i) *Trigonal-bipyramidal structures,*[3,5] *equatorial R, R, S_{th}:* R=alkyl, $\Delta E_{calcd} = -2.94$ mms^{-1}; R = phenyl, $\Delta E_{calcd} = -2.57$ mms^{-1};[3,5] attributable to $Me_2SnCl(SPym)$ (**1a**), $R_2SnCl(SPym)$ (**2–8**), $R_2SnHal(L)$.
(ii) *Octahedral structures,*[3,5] trans-R_2, cis-S_{th}, S_{th}, *cis-N_{het},N_{het}:* R = alkyl, $\Delta E_{calcd} = +2.80$ mm s^{-1}; R = phenyl, $\Delta E_{calcd} = +2.48$ mm s^{-1};[3,5] attributable to $R_2Sn(SPym)_2$ (**9–15**), $R_2Sn(L)_2$.

According to Clark's rule, the environment of tin in $Me_2SnCl(SPym)$ (**1b** and **1c**, Table 3), cannot be assigned a trigonal-bipyramidal structure from the data extracted from idealized regular configurations (*vide supra*). Calculations with bond angles from X-ray crystallography determinations are reported in Fig. 5 I (a–c) and show, for representative species, ΔE_{calcd} data in agreement with the corresponding ΔE_{exp} (*vide supra*) (a word of caution is necessary in this context: pqs parameters employed in the calculations are reliable only for nearly regular structures [20–22,40]). Structure I(a)

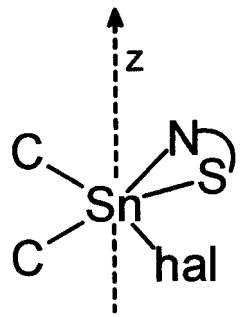

(I)

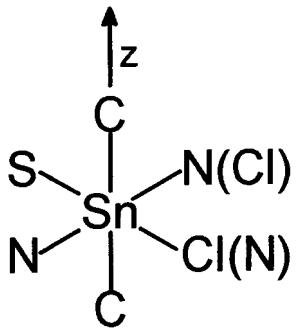

(II)

	Compound	ΔE_{calcd} (mm s^{-1})	Ref.		Compound		ΔE_{calcd} (mm s^{-1})
I(a)	Alk_2SnHal (L)	−3.05	26	II(a)	*trans*-N,N	R = Alk; R = Ph	3.42; 3.10
I(b)	Ph_2SnCl(SPy)	−2.59	5,27	II(b)	*cis*-N,N	R = Alk; R = Ph	3.50; 3.19
I(c)	Ph_2SnCl(TNEE)	−2.42	27				

Figure 5 Point-charge model simulation[20–22] of tin environments. *I*: ΔE_{calcd} for structures from X-ray diffractometry;[5,26,27] Alk = Me, Hal = Cl, L = TNEE; Alk = Et, Hal = Br, L = TNIPE; SPy^- = 2-mercaptopyridine; $TNEE^-$ and $TNIPE^-$ = 2-mercaptopyridine-5-carboxylic acid, ethyl ester (TNEE) and isopropyl ester (TNIPE). See text. II: Me_2SnCl(SPym), **1a–1c**, Table 3, on the assumption of polymeric species by intermolecular interactions through the nitrogen atoms of the ligand (see Fig. 1); idealized octahedral (regular) see structures are assumed. See text.

(Fig. 5) could be attributed to Me_2SnCl(SPym) **1a** and **1b** (Table 3), from Clark's rule, but not to **1c;** additional distortions on I(a), opening the angles C-Sn-C to about 134 °, 141 ° and 145 °, are needed in order to reproduce the ΔE_{exp} data for ΔE_{calcd}. Me_2SnCl(SPym) (**1a–1c**, respectively). On similar grounds, the C-Sn-C angles in Alk_2SnHal(SPym) (**2–7**) would lie between *ca* 128 ° and 132 °. Distortions of the regular trigonal – bipyramidal structures reported in Refs 3 and 5 yield analogous results. Lastly, the *trans*-R_2 octahedral-type structures II (Fig. 5), as extracted from the dynamics of

Table 5 ^{1}H and ^{13}C NMR spectral data for diorganotin(IV) complexes of 2-mercaptopyrimidine:[a] collective ranges of δ (ppm) values[b] in $CDCl_3$ solutions

Compound No.	Formula[a]	δ (ppm)		
^{1}H NMR		H(4,6)[a]		H(5)[a]
1–8	R_2SnHal(SPym)	8.38–8.42 (d)[c]		7.08–7.14 (t)[d]
9–15	$R_2Sn(SPym)_2$	8.24–8.46 (d)[c]		6.83–7.01 (t)[d]
^{13}C NMR		C(2)[a]	C(4,6)[a]	C(5)[a]
1–8	R_2SnHal(SPym)	174.5–176.6[e]	156.9–157.4[f]	115.9–116.7[g]
9–15	$R_2Sn(SPym)_2$	174.5–176.5[e]	156.5–156.8[f]	115.4–115.8[g]

[a] See Fig. 1, labeling of H and C atoms for NMR assignments. R, Hal in classes of complexes: see Table 1. d = doublet; t = triplet.
[b] Tetramethylsilane as internal standard.
[c,d] δ (ppm) in DMSO-d_6 solutions for compounds **5, 8, 9, 11, 13, 15**: (c) 8.48–8.70 d; (d) 7.12–7.39 t. This work, and Ref. 4 for complexes **9, 11, 15**.
[e,f,g] δ (ppm) in DMSO-d_6 solutions for compounds **5, 8, 9, 13, 15:** (e) 172.4–174.0; (f) 157.2–158.5; (g) 116.3–117.0. Ref. 4, complexes **11** and **15:** C(2), 157.4; C(4,6), 120.4, 128.2; C(5), 116.3, 116.7.

tin nuclei (*vide supra*), are attributable to $Me_2SnCl(SPym)$ according to Clark's rule; structures II cannot be assigned to $Ph_2SnCl(SPym)$, while II(a) could be assumed to occur for $Alk_2SnHal(SPym)$ (**2–7**, Table 3), being on the other hand inconsistent with the dynamics of tin in $Cy_2SnBr(SPym)$ (*vide supra*, Table 4).

It is concluded that the solid-state structures of the $R_2Sn(IV)$–SPym complexes investigated here, where the ligand would chelate Sn through S and N donor atoms according to infrared spectroscopic data, are *trans*-Me_2 octahedral or trigonal-bipyramidal in $Me_2SnCl(SPym)$ species, and trigonal-bipyramidal in $R_2SnHal(SPym)$ (R = ^{i}Pr, ^{n}Bu, ^{i}Bu, *t*Bu, Cy, Ph). The complexes $R_2Sn(SPym)_2$ would generally assume *trans*-R_2 octahedral-type structures. Further work is obviously needed for definitive assignments.

Information on structures in solution for complexes **1–15** are extracted from ^{1}H and ^{13}C NMR (Table 5), as well as $^{1}J(^{119}Sn,^{13}C)$ and ^{119}Sn NMR (Table 6); moreover, from IR data in $CDCl_3$ solution, and ^{119}Sn Mössbauer ΔE values in C_2H_5OH, frozen solutions, for $Me_2SnCl(SPym)$ (Tables 2 and 3).

The δ (ppm) values for ligand hydrogen and carbon atoms in complexes $R_2SnHal(SPym)$ and $R_2Sn(SPym)_2$ (Table 5 and Fig. 1) correspond fully to data determined for $RSn(SPym)_3$ and $RSnCl(SPym)_2$ (R = Me, ^{n}Bu, Ph), as well as $RSnCl_2(SPym)$ (R = Me, ^{n}Bu), reported in Ref. 1 [H(4,6), δ = 8.35–8.49 ppm; H(5), δ = 6.91–7.25 ppm; C(2), δ = 172.3–176.9 ppm; C(4,6), = 156.4–157.5 ppm; C(5), δ = 115.7–117.5 ppm]. Structural assumptions extracted for RSn(IV) complexes, on the basis of comparison with data for the disulfide PymSSPym, then hold also for the $R_2Sn(IV)$ species investigated in the present paper: in particular, $SPym^-$ would chelate tin centers through S→Sn and N→Sn coordination in $CDCl_3$ solutions, as well as in DMSO.[1]

Further structural information is extracted from data inherent to $Me_2SnCl(SPym)$. A monomeric undissociated species occurs in $CHCl_3$ solution, according to the experimentally determined molecular weight (Table 1; the same holds for complexes **2–8**); chelation of tin by $SPym^-$ persists in the solution phase ($CDCl_3$), where the IR spectrum shows ν(C–N/C–C) vibrational bands corresponding to solid-state data (footnote e to Table 2). As a consequence, a trigonal-bipyramidal structure of type I (Fig. 5) would occur in $CHCl_3$–$CDCl_3$ solutions. The magnitude of the C-Sn-C angle (ϑ) may be estimated as 123.9 ° through the coupling constant $^{1}J(^{119}Sn,^{13}C)$ in $CDCl_3$ solution (Table 6), according to the treatment by Lockhart and Manders (Eqn [1]):[41]

$$|^{1}J(^{119}Sn,^{13}C)| = 10.7 \times \vartheta - 778 \qquad [1]$$

The same species would occur also in (frozen) C_2H_5OH solution, as extracted from the point-charge model treatment of the ^{119}Sn Mössbauer parameter ΔE_{av} = 3.22 mm s^{-1} (Table 3). In fact, by assuming a trigonal-bipyramidal structure for $Me_2SnCl(SPym)$, from Parish's equation (Eqn 2):[21]

$$\Delta E = -4[R]\{1 - \frac{3}{4}\sin^2\vartheta\}^{1/2} \qquad [2]$$

the value ϑ = C-Sn-C = 125.9 ° is calculated, [R] = 1.13 mm s^{-1} being the partial nuclear quadrupole splitting for equatorial alkyl groups.[21]

Analogous structures could be assumed to occur in $CDCl_3$ solutions for compounds **2–8**, according to the values of the coupling constants $^{1}J(^{119}Sn,^{13}C)$ (Table 6), which, *inter alia*, correspond strictly to data for SPy^- complexes.[5]

Values of δ (ppm) in ^{119}Sn NMR spectra of $R_2SnHal(SPym)$ and $R_2Sn(SPym)_2$ complexes in $CDCl_3$ solutions (Table 6) are in the ranges detected for the corresponding SPy^- complexes, as reported

Table 6 Coupling constants ^{1}J (^{119}Sn, ^{13}C), and ^{119}Sn NMR chemical shifts, δ of diorganotin(IV)-2-mercaptopyrimidine complexes in $CDCl_3$ solution

No.	Compound[(a)] Formula[a]	^{1}J (^{119}Sn, ^{13}C)[(b)] (Hz)	δ (^{119}Sn)[(c)] (ppm)
1	$Me_2SnCl(SPym)$	548	−48
2	$_{i}Pr_2SnCl(SPym)$	491	−66
3	$_{n}Bu_2SnCl(SPym)$	(d)	−53
4	$_{i}Bu_2SnCl(SPym)$	491	−62
5	$_{t}Bu_2SnCl(SPym)$	(d)	−83
6	$Cy_2SnCl(SPym)$	470	−93
7	$Cy_2SnBr(SPym)$	453	−90
8	$Ph_2SnCl(SPym)$	847	−193
9	$Me_2Sn(SPym)_2$	(d)	−107
10	$_{i}Pr_2Sn(SPym)_2$	539	−129
11	$_{n}Bu_2Sn(SPym)_2$	(d)	−111
12	$_{i}Bu_2Sn(SPym)_2$	514	−113
13	$_{t}Bu_2Sn(SPym)_2$	(d)	−57
14	$Cy_2Sn(SPym)_2$	496	−155
15	$Ph_2Sn(SPym)_2$	(d)	−227

[a] Abbreviations: see footnote a to Table 1.
[b] From ^{13}C NMR spectra.
[c] With respect to tetramethyltin as internal standard. $\delta(^{119}Sn)$, (ppm) in DMSO-d_6 solutions: **1**, −114, −138, −224; **5**, −102; **8**, −261. In $CDCl_3$–DMSO-d_6: **9**, −150; **13**, −100; **15**, −259.
[d] Not observed.

in Ref. 5 ($R_2SnCl(SPy)$, R = alkyl and Cy, $\delta = -61$ to -102 ppm; R = Ph, $\delta = -201$ ppm; $R_2Sn(SPy)_2$, R = alkyl and Cy, $\delta = -83$ to -163 ppm; R = Ph, $\delta = -300$ ppm). Shift of δ to higher fields for $R_2SnHal(SPym)$ with respect to $R_2Sn(SPym)_2$ then reflects the decreasing coordination number at tin in the first species, as inferred for the corresponding SPy^- complexes,[5] although the δ ranges do not fit the values reported in the literature for five- and six-coordinated tin derivatives, possibly owing to the large electron-donor ability of sulphur atoms bound to tin.[5] Shifts to lower fields detected in DMSO-d^6, as well as DMSO-d^6–$CDCl_3$, solutions (Table 6, footnote c) could be interpreted in terms of DMSO coordination to tin, according to trends reported for (^{119}Sn) parameters in relation to the increase of the coordination number.[5,42] The occurrence of the species $Ph_2SnCl(SPym)\cdot DMSO$ is suggested by the experimentally determined molecular weight for complex **8**, $Ph_2SnCl(SPym)$, in DMSO solution (Table 1 and footnote d).

CONCLUSIONS

The solid-state structure of complexes $R_2SnHal(SPym)$, (R = $_i$Pr, $_n$Bu, $_i$Bu, $_t$Bu, Cy, Ph) are of trigonal-bipyramidal type, distorted, with angles C-Sn-C larger than 120 ° for $Alk_2Sn(IV)$ and $Cy_2Sn(IV)$ derivatives. Complexes $R_2Sn(SPym)_2$ have *trans*-R_2 octahedral, or better skew-trapezoidal, structures, with *cis*-S,S and *cis*-N,N atoms in the equatorial plane. The complex $Me_2SnCl(SPym)$ could be assumed both as a monomeric, trigonal-bipyramidal, species with the C-Sn-C angle around 134–145 °, or as a monodimensional polymer with a *trans*-R_2 octahedral-type tin environment. These assumptions are extracted from IR, ^{119}Sn Mössbauer, and vtMs studies of tin dynamics. In solution, essentially with $CDCl_3$ as solvent, monomeric species occur, according to vapor pressure osmometry; ligand chelation would persist in solution, and solid-state structures would be maintained, with the exception of $Me_2SnCl(SPym)$, which would assume a distorted trigonal-bipyramidal tin environment for monomeric species. Solution structures are inferred from ^1H,^{13}C,^{119}Sn NMR spectroscopic data, as well as from IR in $CDCl_3$ and ^{119}Sn Mössbauer in frozen C_2H_5OH for $Me_2SnCl(SPym)$.

Acknowledgment The financial support of the Ministero per l'Università e la Ricerca Scientifica (Roma), Fonds der Chemischen Industrie and European Community, is gratefully acknowledged.

REFERENCES

1. F. Huber, R. Schmiedgen, M. Schürmann, R. Barbieri, G. Ruisi and A. Silvestri, *Appl. Organomet. Chem.* **11**, 869 (1997).
2. R. Schmiedgen, F. Huber and M. Schürmann, *Acta Crystallogr. Sect. C* **50**, 391 (1994).
3. A. Barbieri, A. M. Giuliani, G. Ruisi, A. Silvestri and R. Barbieri, *Z. Anorg. Allg. Chem.* **621**, 89 (1995) and reference, therein.
4. D. Kovala Demertzi, P. Tauridou, J. M. Tsangaris and A. Moukarika, *Main Group Met. Chem.* **16**, 315 (1993).
5. R. Schmiedgen, F. Huber, H. Preut, G. Ruisi and R. Barbieri, *Appl. Organomet. Chem.* **8**, 397 (1994) and references therein.
6. J. A. Carbon, L. Hung and D. S. Jones, *Proc. Nat. Acad. Sci. US* **53**, 979 (1965).
7. M. N. Lipsett, *Biochem. Biophys. Res. Commun.* **20**, 224 (1965).
8. J. A. Carbon, H. David and M. H. Studier, *Science* **161**, 1146 (1968).
9. L. Baczynskyj, K. Biemann and R. H. Hall, *Science* **159**, 1481 (1968).
10. M. J. Hynes and M. O'Dowd, *J. Chem. Soc., Dalton Trans.* 563 (1987).
11. M. Boualam, J. Meunier-Piret, M. Biesemans, R. Willem and M. Gielen, *Inorg. Chim. Acta* **198–200**, 249 (1992).
12. E. Krause and R. Pohland, *Ber. Dtsch. Chem. Ges.* **57**, 532 (1924).
13. W. J. Jones, W. C. Davies, S. T. Bowden, C. Edwards, V. E. Davis and L. H. Thomas, *J. Chem. Soc.* 1446 (1947).
14. H. Gilman and L. A. Gist Jr., *J. Org. Chem.* **22**, 368 (1957).
15. S. A. Kandil and A. L. Allred, *J. Chem. Soc. A* 2987 (1970).
16. D. D. Perrin and W. L. F. Armarego, *Purification of Laboratory Chemicals*, 3rd edn, Pergamon Press, Oxford, 1988.
17. B. Wurzschmitt, *Mikrochim. Acta* **36–37**, 769 (1951).
18. R. Barbieri and M. T. Musmeci, *J. Inorg. Biochem.* **32**, 89 (1988).
19. R. Barbieri, G. Ruisi, A. Silvestri, A. M. Giuliani, A. Barbieri, G. Spina, F. Pieralli and F. Del Giallo, *J. Chem. Soc., Dalton Trans.* 467 (1995) and references therein.
20. G. M. Bancroft and R. H. Platt, Adv. Inorg. Chem. Radiochem.**15**, 59 (1972).
21. R. V. Parish, Structure and bonding in tin compounds. In: *Mössbauer Spectroscopy Applied to Inorganic Chemistry*, Long, G. J. (ed.), Plenum Press, New York, 1984, Vol. 1, Ch. 16, p. 527.
22. R. Barbieri, F. Huber, L. Pellerito, G. Ruisi and A. Silvestri, ^{119m}Sn Mössbauer studies on tin compounds. In: *Chemistry of Tin*, Smith, P. J. (ed.), Blackie Academic and Professional, London, 1997, Ch. 14, p. 496.
23. B. Kolk, Studies of dynamical properties of solids with the

Mössbauer effect. In: *Dynamical Properties of Solids*, Horton, G. K. and Maradudin, A. A. (eds), North-Holland, Amsterdam, 1984, Vol. 5, Ch. 1, p. 3.
24. R. H. Herber, Structure, bonding, and the Mössbauer lattice temperature. In: *Chemical Mössbauer Spectroscopy*, Herber, R. H. (ed.), Plenum Press, New York, 1984, Ch. 8, p. 199.
25. E. R. Bauminger and I. Nowick, The dynamics of nuclei studied by Mössbauer spectroscopy. In: *Mössbauer Spectroscopy*, Dickson, D. P. E. and Berry, F. J. (eds.), Cambridge University Press, Cambridge, 1986, Ch. 6, p. 219.
26. M. D. Couce, G. Faraglia, U. Russo, L. Sindellari and G. Valle, *J. Organomet. Chem.* **513**, 77 (1996).
27. M. D. Couce, V. Cherchi, G. Faraglia, U. Russo, L. Sindellari, G. Valle and N. Zancan, *Appl. Organomet. Chem.* **10**, 35 (1996).
28. F. P. Mullins, *J. Inorg. Nucl. Chem.* **41**, 463 (1979).
29. E. Kellö, V. Vrabel, A. Lycka and J. Sivy, *Acta Crystallogr. Sect. C* **49**, 1943 (1993).
30. M. V. Castaño, A. Macias, A. Castiñeiras, A. Sánchez Gonzáles, E. Garcia Martinez, J. S. Casas, J. Sordo, W. Hiller and E. E. Castellano, *J. Chem. Soc., Dalton Trans.* 1001 (1990).
31. M. D. Couce, G. Faraglia, U. Russo and G. Valle, *Z. Kristallogr.* **211**, 509 (1996).
32. M. D. Couce, G. Faraglia, U. Russo and G. Valle, *J. Chem. Crystallogr.* **26**, 479 (1996).
33. G. Domazetis, B. D. James, M. F. Mc Kay and R. J. Magee, *J. Inorg. Nucl. Chem.* **41**, 1555 (1979).
34. R. Schmiedgen, F. Huber and H. Preut, *Acta Crystallogr. Sect. C* **49**, 1735 (1993).
35. T. K. Sham and G. M. Bancroft, *Inorg. Chem.* **14**, 2281 (1975).
36. R. Barbieri, A. Silvestri, A. Barbieri, G. Ruisi, F. Huber and C.-D. Hager, *Gazz. Chim. Ital.* **124**, 187 (1994), and references therein.
37. S. Matsubara, M. Katada, K. Sato, I. Motoyama and H. Sano, *J. Phys.* **40**, C2-363 (1979).
38. H. Sano and Y. Mekata, *Chem. Lett.* 155 (1975).
39. G. C. Stocco, L. Pellerito, M. A. Girasolo and A. G. Osborne, *Inorg. Chim. Acta* **83**, 79 (1984).
40. M. G. Clark, A. G. Maddock and R. H. Platt, *J. Chem. Soc., Dalton Trans.* 281 (1972).
41. T. P. Lockhart and W. F. Manders, *J. Am. Chem. Soc.* **109**, 7015 (1987).
42. J. Otera, *J. Organomet. Chem.* **221**, 57 (1981).

